

University of Groningen

Local magnetism in rare-earth metals encapsulated in fullerenes

De Nadai, C; Mirone, A; Dhesi, SS; Bencok, P; Brookes, NB; Marenne, [No Value]; Rudolf, Petra; Tagmatarchis, N; Shinohara, H; Dennis, TJS

Published in:
Physical Review. B: Condensed Matter and Materials Physics

DOI:
[10.1103/PhysRevB.69.184421](https://doi.org/10.1103/PhysRevB.69.184421)

IMPORTANT NOTE: You are advised to consult the publisher's version (publisher's PDF) if you wish to cite from it. Please check the document version below.

Document Version
Publisher's PDF, also known as Version of record

Publication date:
2004

[Link to publication in University of Groningen/UMCG research database](#)

Citation for published version (APA):

De Nadai, C., Mirone, A., Dhesi, S. S., Bencok, P., Brookes, N. B., Marenne, . N. V., ... Nadaï, C. D. (2004). Local magnetism in rare-earth metals encapsulated in fullerenes. *Physical Review. B: Condensed Matter and Materials Physics*, 69(18), [184421]. DOI: 10.1103/PhysRevB.69.184421

Copyright

Other than for strictly personal use, it is not permitted to download or to forward/distribute the text or part of it without the consent of the author(s) and/or copyright holder(s), unless the work is under an open content license (like Creative Commons).

Take-down policy

If you believe that this document breaches copyright please contact us providing details, and we will remove access to the work immediately and investigate your claim.

Downloaded from the University of Groningen/UMCG research database (Pure): <http://www.rug.nl/research/portal>. For technical reasons the number of authors shown on this cover page is limited to 10 maximum.

Local magnetism in rare-earth metals encapsulated in fullerenesC. De Nadai, A. Mirone, S. S. Dhesi,* P. Bencok, and N. B. Brookes
*European Synchrotron Radiation Facility, Boîte Postale 220, 38043 Grenoble, France*I. Marenne
*Facultés Universitaires Notre-Dame de la Paix, Rue de Bruxelles 61, 5000 Namur, Belgium*P. Rudolf
*Materials Science Centre, University of Groningen, Nijenborgh 4 9747 AG Groningen, The Netherlands*N. Tagmatarchis and H. Shinohara
*Department of Chemistry, Nagoya University, Nagoya 464-8602, Japan*T. J. S. Dennis
Department of Chemistry, Queen Mary, University of London, Mile End Road, London E1 4NS, United Kingdom
(Received 28 November 2003; published 28 May 2004)

Local magnetic properties of rare-earth (RE) atoms encapsulated in fullerenes have been characterized using x-ray magnetic circular dichroism and x-ray absorption spectroscopy (XAS). The orbital and spin contributions of the magnetic moment have been determined through sum rules and theoretical model calculations, and have been found to be highly reduced compared to those of the corresponding *free* RE³⁺ ions. Crystal-field and hybridization effects have been investigated by the way of calculations to simulate the effect of the carbon cage on the RE; both hypotheses have reproduced the experimental spectra resulting also in a significant reduction of the orbital and spin moments. While isotropic XAS spectra have confirmed a roughly trivalent state for the RE metals, a back electron transfer from the cage to the metal has been quantified. A paramagnetic coupling has been found between the metal centers from 6 K to 300 K.

DOI: 10.1103/PhysRevB.69.184421

PACS number(s): 75.75.+a, 71.20.Tx, 73.22.-f, 78.70.Dm

I. INTRODUCTION

Endohedral metallofullerenes $M@C_{82}$ are novel materials. Their structural, electronic, and solid-states properties have attracted a wide interest not only in physics and chemistry but also in materials or biological sciences with a large variety of promising applications, as has recently been reviewed.¹⁻³ In endohedral metallofullerenes, a positively charged core metal is off-center in a negatively charged strong carbon cage, resulting in strong metal-cage interaction and intrafullerene charge transfer from the metal to the cage.^{2,4-6} The consequent electric dipole moment occurring along the symmetry axis of the $M@C_{82}$ molecules implies a particular molecular arrangement in a “head-to-tail” manner (linear or ring-shaped configurations) in crystals and on metal surfaces.^{4,7-9} These unusual molecular and electronic structures are expected to be at the origin of novel properties.

The study of magnetism of these systems has been taken up recently. Some superconducting quantum interference device (SQUID) magnetometry and electron spin resonance measurements have been made on $M@C_{82}$ ($M=La, Ce, Gd,$ and Eu) reporting a paramagnetic behavior between 7 and 300 K.¹⁰⁻¹² Nevertheless, intermetallofullerene ferromagnetic coupling has been mentioned at sub-20-K for heavy rare-earth (RE) endofullerenes.¹³ An interesting evolution of the effective paramagnetic moment (μ_{eff}) has also been reported. First in $Ce@C_{82}$ μ_{eff} is found to decrease with temperature from $2.3\mu_B$ at 300 K to $1.0\mu_B$ at 2 K.¹¹ Then, whereas in $La@C_{82}$ the average μ_{eff} of La^{3+} ion has been

found larger than the theoretical value¹⁰ due to an incomplete electron transfer from the metal to the cage,¹⁴ it appears dramatically smaller in heavy RE metallofullerenes $M@C_{82}$ (e.g., $Ho@C_{82}$, $6.3\mu_B$; theoretical Ho^{3+} , $10.6\mu_B$; Ho^{2+} , $9.5\mu_B$).¹³ The general trend is that the higher the RE orbital moment (L), the more μ_{eff} is reduced. It is recognized that when dealing with magnetism of lanthanide metal-containing compounds, the orbital angular momentum plays an important role.¹⁵ Here the carbon cage crystal field and orbital hybridization may partially quench the RE orbital moment due to the very low symmetry.

At present, a direct observation of the local electronic and magnetic structures of the encapsulated metal is essential to study any intermolecular magnetic ordering and to understand the origin of the reduced μ_{eff} , observed even in $Gd@C_{82}$ where $L=0$. X-ray absorption spectroscopy (XAS) and x-ray magnetic circular dichroism (XMCD) are ideal techniques to investigate electronic and magnetic properties of endohedral metallofullerenes since these high-energy spectroscopies are able to deal with quite small quantities of material. This is a significant advantage considering the time-consuming nature of the extraction of pure endohedral fullerenes from mixed (metallo)fullerene soot using multi-cycle high-performance liquid chromatography and the consequent scarcity of the highly pure fullerene material required for high-level research. In addition, with these absorption techniques, it is possible to determine element-specific properties in a composite system such as endohedral fullerenes. With the advent of high-brilliance polarized soft

x-ray sources, XMCD has been developed into a unique probe of the ground-state spin \mathbf{S} and orbital \mathbf{L} magnetic moments through the use of sum rules.^{16,17}

In the present study, the local magnetism of RE atoms encapsulated in fullerenes is investigated. The XMCD sum rules are applied to $M@C_{82}$ molecules ($M = \text{Gd}, \text{Dy}, \text{Ho}$) and $\text{Er}_2@C_{90}$ to extract the orbital contribution of the encaged-metal magnetic moment. As the applicability of the spin sum rules in such systems is difficult, the spin moment is studied through atomic calculations. Two models are used to reproduce the experimental results in terms of crystal-field (CF) and hybridization effects. The $4f$ \mathbf{L} and \mathbf{S} moments and the magnetic ordering at low temperature between the metal centers are discussed in order to clarify the influence of the carbon cage on the metal atom and therefore the large reduction of the total magnetic moment observed for encapsulated heavy-RE.

II. EXPERIMENT

The isomer pure metallofullerenes were synthesized as described in Refs. 18–20, or obtained commercially ($M = \text{Ho}$). Measurements were performed on *in situ* prepared $M@C_{82}/\text{Cu}(111)$ samples. The $\text{Cu}(111)$ substrate was cleaned by repeated cycles of Ar^+ sputtering and annealing to 700 K in ultrahigh vacuum (UHV). The molecules were sublimed from an alumina crucible onto $\text{Cu}(111)$ at room temperature with a base pressure of 1×10^{-9} mbar. For this purpose, a resistively heated effusion cell, operating between 873 K and 930 K, has been specially designed to cope with the small quantities of material involved. The relative thickness of the films (>3 ML) was followed using the edge jump in the XAS spectra and scanning tunneling microscopy calibration. A high flux ($\sim 10^{13}$ photon/s/0.1% BW) of $\sim 100\%$ polarized soft x rays at the sample was obtained from beamline ID08 which provides full polarization control using an APPLE II helical undulator at the European Synchrotron Radiation Facility (ESRF) in Grenoble. XMCD measurements were performed using a 7 T superconducting magnet in UHV environment. The XMCD was determined by switching both the sample magnetization \mathbf{M} and the polarization vector of the incident radiation, \mathbf{P} , to remove any systematic errors. The measurements were carried out in total electron yield detection mode, both at normal and grazing incidence, i.e., with the incident photon beam at $\theta = 90^\circ$ and 30° from the sample surface in order to study any magnetic anisotropy. The pressure in the magnet chamber was 1×10^{-10} mbar with all measurements done in the temperature range from 6 K to 293 K.

III. THEORETICAL MODEL

The ligand-field atomic-multiplet theory has been used to calculate the multiplet structure of core-to- $4f$ excitations in RE.²¹ This theory is based on the same essential physical assumptions as that of the ligand-field atomic model developed by Thole and co-workers^{22–24} with the advantage of being applicable to any geometry regardless of the ligand-field symmetry group. The electrostatic interactions and ex-

change parameters used in the present work were taken from Ref. 25 considering the 80% reduction factor of the core-valence and valence-valence Slater's integrals to simulate solid effects at the atomic level. Two different models were considered, one with a CF splitting and the other with a term describing the hopping from the cage to the RE $4f$ shell. The considered Hamiltonian for the CF model is

$$H_{atomic} + \sum_{\eta\sigma} E_{\eta} f_{\eta\sigma}^{\dagger} f_{\eta\sigma}, \quad (1)$$

where H_{atomic} describes the electronic structure of the atom-like RE as in Ref. 25, and the second term represents the CF perturbation. In such CF term, f^{\dagger}/f are creation/annihilation operators and η runs over the $4f$ orbitals [$4f_{x(x^2-3y^2)}$, $4f_{(3x^2-y^2)y}$, $4f_{xyz}$, $4f_{(x^2-y^2)z}$, $4f_{xz^2}$, $4f_{yz^2}$, and $4f_{z^3}$]. The parameters E_{η} satisfy the constraint $E_{yz^2} = E_{xz^2}$, $E_{(x^2-y^2)z} = E_{xyz}$, $E_{x(x^2-3y^2)} = E_{(3x^2-y^2)y}$ to ensure axial symmetry along the z axis. In this way we try to simulate roughly the atomic environment of the off-centered RE ions inside the cage with the decentering direction along the z axis. For the model with hybridization, a hopping term between the $4f$ orbitals of the lanthanide and the valence orbitals of the carbon cage has been considered. The Hamiltonian is described by

$$H_{atomic} + t \sum_{\eta\sigma} (f_{\eta\sigma}^{\dagger} c_{v\sigma} + c_{v\sigma}^{\dagger} f_{\eta\sigma}) - \Delta E \sum_{\sigma} c_{v\sigma}^{\dagger} c_{v\sigma}, \quad (2)$$

where c^{\dagger}/c are creation/annihilation operators for the cage orbitals, and the two free parameters are the hopping strength t and ΔE which governs the ground-state average valence as explained below. In this model the cage valence orbital interacting through hybridization with the $4f$ orbitals is non-degenerate and the transition term does not commute with angular momentum. In the hybridization model, the ground state can be described as $3d^{10}(4f, c)^{n+1}$ where n is the RE electron number (7, 9, 10, and 11 for Gd^{3+} , Dy^{3+} , Ho^{3+} , and Er^{3+} respectively), and c represents the cage orbitals. Calculations are limited to consider configurations where cage orbitals host one or zero electron. The parameter ΔE separates the center of mass of $4f^n c^1$ multiplets from the one of $4f^{n+1} c^0$. The large negative ΔE value ensures that the ground state is mainly $4f^n c^1$ with a small $4f^{n+1} c^0$ components. The excited state is $3d^9(4f, c)^{n+2}$. For the CF model, the ground and excited configurations are $3d^{10}4f^n$ and $3d^94f^{n+1}$, respectively. For the calculations of XAS spectra, two matrices were considered, namely, M_g for the ground-state Hamiltonian and M_e for the excited state. The ground state $|g\rangle$ was found using the Lanczos method, while the scattering factors were deduced from the dipole-dipole correlation function

$$D_{ij}(\omega) = \langle g | D_i \frac{1}{(\omega - M_e + i\Gamma)} D_j | g \rangle, \quad (3)$$

where D_i is the dipole operator and Γ is the lifetime broadening.

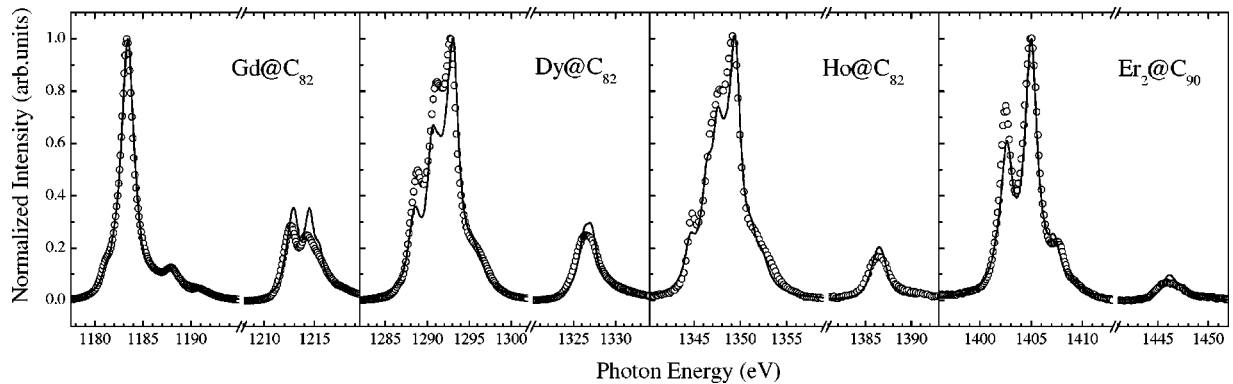


FIG. 1. RE $M_{4,5}$ XAS measured at normal incidence with respect to the sample surface (open circles). The spectra are normalized to a constant edge jump. The atomic calculations for the respective free ion (RE^{3+}) are shown as solid lines.

IV. RESULTS AND DISCUSSION

A few studies on the charge transfer from the metal to the cage have already been published, mostly for the filled and half-filled $4f$ shell RE atoms. XAS, electron-energy-loss spectroscopy, and resonant photoemission measurements on Gd@C_{82} have reported a half-filled $4f^7$ initial state configuration.^{5,26,27} Results on the other RE oxidation state are rarer. Dy@C_{82} has been studied with XAS resulting in a Dy^{3+} ion by comparison with Dy_2O_3 ,⁶ and an x-ray photoemission spectroscopy study of Ho@C_{82} has reported Ho ion in an approximately trivalent state by comparison with $\text{HoCl}_3 \cdot 6\text{H}_2\text{O}$.²⁸

All the endohedral metallofullerene films prepared here have been first studied with XAS to probe the electronic structure of the encapsulated metal. The isotropic RE $M_{4,5}$ edges recorded at normal incidence with respect to the samples surface are shown in Fig. 1 (open circle). Atomic multiplet calculations have been used to simulate the $3d$ x-ray absorption lines of the whole series of RE metals.²⁵ We reproduced in Fig. 1 (full line) the trivalent lanthanide spectra for direct comparison with the respective encapsulated ion. The spectra show a multiplet structure due to electric-dipole transitions from the $3d$ core level to the unoccupied $4f$ levels. In all cases, the agreement between experimental and theoretical spectra is very good and many similarities with the respective RE_2O_3 XAS spectra are found in the literature.²⁹ This confirms the trivalent nature of the RE studied here in monometallofullerenes and dimetallofullerenes in concordance with the previous work.^{5,6,26–28} Nevertheless, three points deserve further discussion. First, for Gd@C_{82} and Dy@C_{82} , the branching ratio $I(M_5)/[I(M_4) + I(M_5)]$ is larger than the calculated one considering the Hund's rule ground state. Generally a larger branching ratio corresponds to a higher spin state,³⁰ but in the particular case of gadolinium this is not possible as \mathbf{S} is already maximum ($S = \frac{7}{2}$ for Gd^{3+}). In addition, the discrepancy in the intensity ratio of the two M_4 peaks has already been observed for Gd_2O_3 .^{25,26,29} Also Dy@C_{82} presents a slightly different line shape from Dy_2O_3 (Ref. 29) when comparing the intensity ratios of the three first structures within M_5 edge (Dy@C_{82} , 0.5/0.83/1; Dy_2O_3 (Ref. 29), 0.43/0.77/1; Dy^{3+} calculation, 0.3/0.6/1). The higher intensity of the two first peaks in

Dy@C_{82} is opposite to the expected evolution of the line shape going from a $4f^9$ towards a $4f^{10}$ configuration—which could explain a larger branching ratio—as can be seen in the multiplet calculations by comparing Dy^{3+} and Ho^{3+} .²⁵ In addition, no broadening of the peaks occurs as would be expected in the case of a mixed valence since the energy resolution (0.6 eV) is lower than the expected shift (1.7 eV). This intensity discrepancy is not attributed to a hybridization effect, but more to a “substrate” effect that has been observed experimentally depending on the coverage.³¹ Finally, the first M_5 structure in $\text{Er}_2@C_{90}$ is poorly reproduced by the calculation as already observed in the case of Er_2O_3 .²⁵

In order to determine the local magnetic properties of the RE ion within the carbon cage we used XMCD. The top panels of Fig. 2 show RE $M_{4,5}$ XAS spectra recorded at a temperature of 6 K with \mathbf{M} parallel (open circle) and anti-parallel (solid circle) to \mathbf{P} . For all the series, except gadolinium that looks atomiclike, the circularly polarized XAS spectra are rather complicated giving rise to numerous structures in the M_5 region that are absent in the calculated spectra of the *free* trivalent ions.³² The difference between these two XAS spectra, i.e., the XMCD, is displayed in the respective bottom panels of Fig. 2. In the first two bottom panels chosen as examples, the insets show the integral of the respective XMCD spectrum indicating the integral over the M_5 edge (ΔA_5) and the integral over the M_4 edge (ΔA_4). First of all, the intermolecular magnetic coupling between the entrapped metal centers can be determined by following the temperature and field dependence of XMCD. All the metallofullerenes investigated here exhibit a similar behavior. The temperature dependence of the XMCD signal, from 6 K to 300 K, did not show any evolution of the line shape, but only a decrease of its intensity, indicative of paramagnetic behavior. We have also followed the field dependence of the measured M_5 dichroism maximum. No open hysteresis loop has been observed for any molecules even at 6 K. Only a paramagnetic coupling can be concluded from these measurements, providing no evidence of any low-temperature ferromagnetic coupling between the entrapped metals as suggested by previous studies.¹³

The sum rules relate the intensity of the XMCD signal to the ground-state expectation value of the magnetic field op-

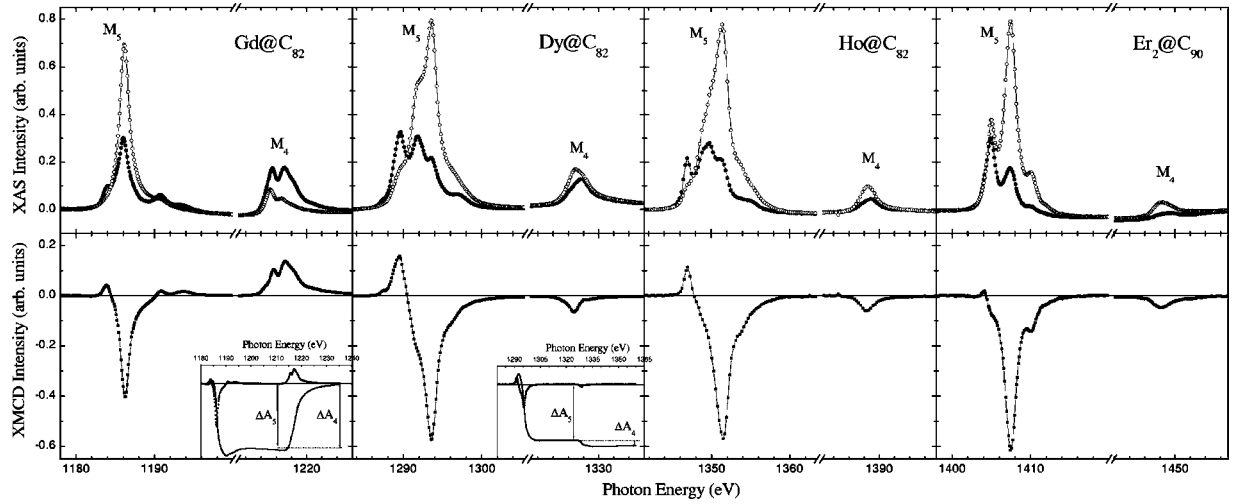


FIG. 2. Top panels: RE $M_{4,5}$ XAS spectra recorded with \mathbf{M} parallel (open circle) and antiparallel (solid circle) to \mathbf{P} at normal incidence with respect to the sample surface; the spectra are normalized to the same factor as the sum XAS shown in Fig. 1. Bottom panels: the difference between the two spectra shown in the respective top panels is the XMCD; in the first two panels chosen as examples, the inset shows the integral of the respective XMCD spectrum indicating the integral over the M_5 edge (ΔA_5) and the integral over the M_4 edge (ΔA_4) used to determine \mathbf{L} through sum rules.

erators (orbital $\langle L_z \rangle$, spin $\langle S_z \rangle$, and magnetic dipole $\langle T_z \rangle$) of the valence electrons.^{16,17} The intensity of the XMCD signal, integrated over a complete core-level edge and normalized to the isotropic XAS spectrum, yields the ground-state expectation value of the orbital angular momentum per hole.¹⁶ At the RE $M_{4,5}$ edges, the orbital momentum $\langle L_z \rangle^{4f}$ is given by

$$\langle L_z \rangle = -2 \frac{\Delta A_5 + \Delta A_4}{A_5 + A_4} n_h^{4f}, \quad (4)$$

where n_h^{4f} represents the number of holes on the $4f$ localized orbital of the RE ion, $(\Delta A_5 + \Delta A_4)$ is the integral over $M_{4,5}$ edges of the XMCD (as shown in the insets of Fig. 2), and $(A_5 + A_4)$ is the integrated sum spectrum. The strong spin-orbit coupling in the $5d$ ions makes the spin sum rule¹⁷ difficult to apply to these systems because of a rather large $\langle T_z \rangle$ term. For this reason $\langle S_z \rangle$ has been determined by the way of atomic calculations.

The $\langle L_z \rangle_{exp}$ values extracted from the experiment by applying the sum rules are listed in Table I. The theoretical values expected for the *free* RE^{3+} ions in the atomic limit are also reported for comparison. Gd@C₈₂ has been used as a reference here. The trivalent Gd³⁺ is supposed to have a

half-filled $4f$ shell that yields zero orbital moment. Indeed, the integral over $M_{4,5}$ edges returns to zero within the error bars. For the other RE ions, $\langle L_z \rangle$ is strongly reduced compared to the theoretical values expected for a *free* RE^{3+} ion, from $\sim 46\%$ to $\sim 53\%$ as can be seen in Table I. First this reduction cannot be related to a lack of magnetic saturation of the films as they were found to be magnetically saturated at $\sim 95\%$ at the working conditions of 7 T. This value was determined through fitting of the hysteresis curves [$XMCD = f(H)$] using a Brillouin function. Then a similar phenomenon concerning the total effective magnetic moment μ_{eff} of these molecules has already been reported.¹³ Such reductions of μ_{eff} from 20% in Dy@C₈₂ to 47.6% in Ho@C₈₂ and 33.5% in Er@C₈₂ have been suggested as arising from a partial quenching of \mathbf{L} of the metal due to the carbon cage CF and to a possible back electron transfer from the cage to the metal $5d$ orbitals.¹³

Our work shows indeed that $\langle L_z \rangle$ is strongly affected by the presence of the carbon cage and in the same proportion as μ_{eff} for Ho@C₈₂ and Er@C₈₂; in the last case, the percentage of reduction in $\langle L_z \rangle$ for Er³⁺ in the monometallofullerene Er@C₈₂ is expected to be smaller than in the measured dimetallofullerene Er₂@C₉₀. This is a general rule

TABLE I. Experimental and calculated orbital and spin moments for the RE ion encapsulated in the fullerene.

Ion	$\langle L_z \rangle_{n_h}$	Sum rule			Calculations				Reduction of L_z	$\langle S_z \rangle_{th}$	Δn	
		$\langle L_z \rangle_{exp}$	Reduction of L_z	$\langle L_z \rangle_{th}$	$\langle L_z \rangle_{calc}^{CF}$	$\langle L_z \rangle_{calc}^{HYB}$	$\langle S_z \rangle_{calc}^{CF}$	$\langle S_z \rangle_{calc}^{HYB}$				Reduction of S_z
Gd@C ₈₂	-0.01(2)	-0.1(2)		0	-0.04	-0.03	-3.46/-2.8	-2.86	20%	$\frac{7}{2}$	0.04	
Dy@C ₈₂	-0.53(5)	-2.7(3)	46%	5	-2.43	-2.45	-1.22	-1.21	51%	51%	$\frac{5}{2}$	0.013
Ho@C ₈₂	-0.69(7)	-2.8(3)	53%	6	-2.99	-3.12	-1.0	-1.01	49%	50%	2	0.008
Er ₂ @C ₉₀	-0.92(9)	-2.8(3)	53%	6	-2.80 ^a	-2.64 ^a	-0.70 ^a	-0.66 ^a	55% ^a	53% ^a	$\frac{3}{2}$	0.007 ^a

^aCalculations have reproduced Er₂@C₉₀ spectra while considering a monometallofullerene of Er@C₈₂ type.

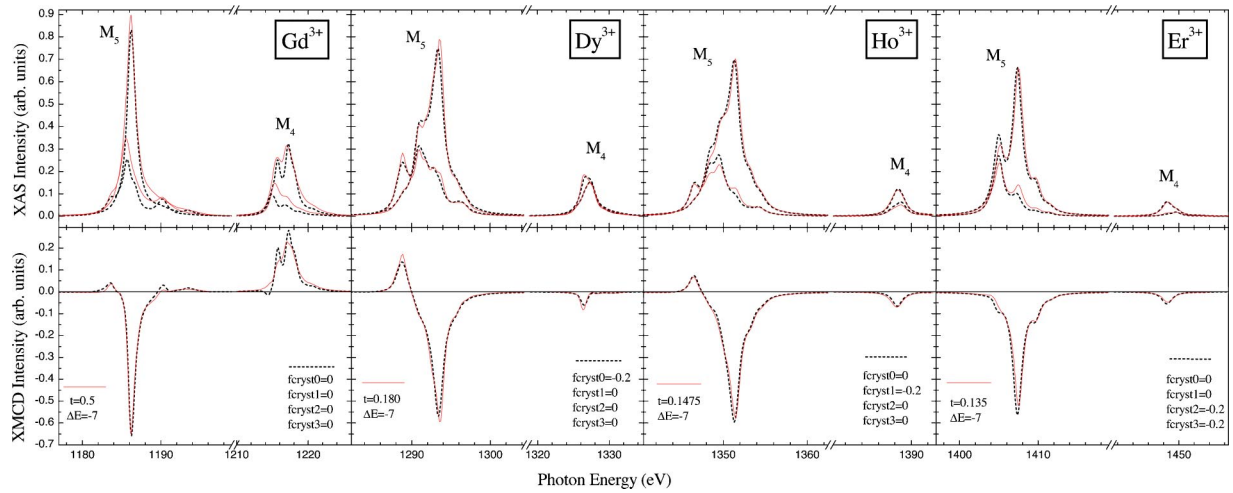


FIG. 3. (Color online) Top panels: theoretical RE $M_{4,5}$ XAS spectra calculated considering a crystal-field splitting (dotted lines) and orbitals hybridization between the cage and the RE (solid lines). Bottom panels: the differences between the two XAS spectra shown in the respective top panel, i.e., calculated XMCD; the parameters used in the calculations are also reported.

observed when going from an isolated atom to clusters and solids, and it has also been observed in the comparison between $\text{Dy}@C_{82}$ and $\text{Dy}_2@C_{92}$ where 10% more reduced $\langle L_z \rangle$ has been obtained for the dimetallofullerene.³¹ But in $\text{Dy}@C_{82}$ the reduction found for $\langle L_z \rangle$ is more than double compared to μ_{eff} in SQUID measurements. This disagreement could partially be explained by the branching-ratio problem observed already with XAS, as a smaller M_5 intensity with respect to M_4 would give a higher $\langle L_z \rangle$. However, there still remains a question about the origin of these moments' reduction: can this be a CF quenching of \mathbf{L} since RE are known to not be very sensitive to CF, and is \mathbf{S} also affected by the presence of the carbon cage?

Theoretical calculations provide a good way of extracting \mathbf{L} and \mathbf{S} and also of understanding the origin of this phenomenon by simulation of CF and hybridization effects. The quenching of \mathbf{L} by the fullerene CF splitting has been tested first. The calculated XAS spectra and the respective dichroism for the monometallofullerenes $M@C_{82}$ ($M=\text{Gd}, \text{Dy}, \text{Ho}, \text{Er}$) are shown in Fig. 3 (dotted lines). Starting from the atomic state of the M^{3+} ion, the relative energy positions of the m_l components have been tested to reproduce the degeneracy breaking of the $4f$ orbitals ($4f_{x(x^2-3y^2)}$, $4f_{(3x^2-y^2)y}$, $4f_{xyz}$, $4f_{(x^2-y^2)z}$, $4f_{xz^2}$, $4f_{yz^2}$, and $4f_{z^3}$). The results are reported in the respective panels (fcryst values). In the special case of gadolinium, showing atomlike spectra, the addition of any CF splitting did not change the line shape of the spectra, as expected for the spherical symmetry of a fully-degenerated half-filled $4f$ shell. The resulting $\langle L_z \rangle_{calc}^{CF}$ and $\langle S_z \rangle_{calc}^{CF}$ moments, reported in Table I, show no reduction compared to the atomlike moments. Nevertheless, it is important to observe that the intensity of the XMCD with respect to the sum is poorly reproduced by the calculations, showing $\sim 20\%$ difference between the experiment and the calculation when we correct the M_5 edge for the branching-ratio discrepancy mentioned above. This can be directly related to a 20% reduced $\langle S_z \rangle$ as $\langle L_z \rangle=0$ and $\langle T_z \rangle$ is supposed to be zero for Gd^{3+} , but it cannot be explained by this CF

model. Then for the other RE metallofullerenes, the line shape and intensities of the various structures of the experimental spectra have been well reproduced using ~ 0.2 eV CF splitting. This small value reflects the low sensitivity of the RE to the CF compared to the spin-orbit interaction $\zeta\langle \mathbf{L} \cdot \mathbf{S} \rangle$ [where $\zeta_f(\text{Dy})=0.246$ eV, $\zeta_f(\text{Er})=0.302$ eV at the ground state]. Moreover, the calculations have determined the splitting to be localized on a particular $4f$ orbital depending on the studied RE. Nevertheless, the calculated localization of the CF splitting has been found dependent of the beam and applied magnetic field direction. Indeed, the relative energy positions of the m_l orbitals reported in Fig. 3 have been calculated considering the applied magnetic field and the light direction along the z axis of the $4f$ orbitals. When applying a 90° rotation of the beam and magnetic field direction, the splitting follows this rotation: for instance, in the case of Dy the lowest orbitals are found to be $4f_{x(x^2-3y^2)}$ and $4f_{(3x^2-y^2)y}$ ($m_l=3$), i.e., the orbitals at 90° of $4f_{z^3}$ ($m_l=0$) obtained in the presented calculations. In addition, experimentally the molecules have shown no particular orientation in the thick films. Indeed additional measurements at grazing incidence ($\theta=30^\circ$) have shown no significant in-plane/out-of-plane anisotropy for all the molecules.³¹ In fact the molecules are known to interact in a head-to-tail manner (ring-shaped configuration) but they can form orientated domains on the Cu(111) surface with different directions resulting in an average orientation within the measured area. In this probable configuration no orbital anisotropy can be measured. So we believe that the particular orientations of the CF splitting should not be interpreted in the present case. More important is the good simulation of the experimental spectra and the resulting magnetic moments. The $\langle L_z \rangle_{calc}^{CF}$ and $\langle S_z \rangle_{calc}^{CF}$ moments calculated from these configurations are reported in Table I for each molecule. First $\langle L_z \rangle_{calc}^{CF}$ is in good agreement with $\langle L_z \rangle_{exp}$, confirming the strong reduction observed experimentally. Second, $\langle S_z \rangle_{calc}^{CF}$ also shows a significant decrease compared to the atomlike M^{3+} values. It is interesting to note that the

ratio $\langle L_z \rangle / \langle S_z \rangle$ is equal to the theoretical value, meaning that $\langle S_z \rangle$ is as much reduced as $\langle L_z \rangle$, and the resulting \mathbf{L} and \mathbf{S} stay parallel as expected for heavy RE atoms. This has already been demonstrated within sum rules in jj -coupled operators in the case of lanthanides and actinides.³³ The rule implies that in intermediate coupling the ratios of the $\langle L_z \rangle$, $\langle S_z \rangle$, and $\langle T_z \rangle$ operators with the same total moment are fixed as long as the perturbation (here the CF) is smaller than the electrostatic and spin-orbit interactions. The CF model therefore provides a good way to simulate the experimental spectra giving a strongly reduced $\langle L_z \rangle$ in agreement with the sum rules. However, $\langle S_z \rangle$ is also reduced. This indicates that the μ_{eff} reduction seen by SQUID cannot be explained only by a quenching of \mathbf{L} by the carbon cage crystal field.

In order to understand more fully the reduction in \mathbf{S} , theoretical calculations were also used to investigate the effect of hybridization between the carbon cage and the RE $4f$ orbitals as described in Sec. III. The resulting calculated spectra are shown in Fig. 3 (solid lines) with the two free parameters of this model, t and ΔE , reported in the respective panels. Unlike in the CF model, Gd@C₈₂ spectra were well reproduced using a charge transfer back from the cage to Gd³⁺. Despite the XAS intensity discrepancy at the M_5 edge that still remains due to the anomalous branching ratio, the calculated XAS and XMCD spectra are in good agreement with the experiment. The resulting $\langle S_z \rangle_{calc}^{HYB}$ was found to be 20% smaller than the theoretical value ($\frac{7}{2}$), exactly as described in the preceding paragraph after direct comparison of the *atomic* calculation with the experiment. This unexpected $\langle S_z \rangle$ reduction for Gd is probably at the origin of the μ_{eff} reduction observed by SQUID for Gd@C₈₂.¹³ For all other metallofullerenes, the calculated spectra are very close to those calculated with the CF model, and are also in very good agreement with the experiment. t and ΔE were found to be strongly correlated and the calculated spectra were found to depend mainly on the hopping term and the average occupancy $1-\Delta n$ of the v orbital, as Δn is found to vary continuously with t . Indeed, the moments reduction was found to be linked to the hopping term value as no reduction occurs if $t=0$ and the reduction increases for incremented t . The respective values of Δn are given in Table I with the resulting $\langle L_z \rangle_{calc}^{HYB}$ and $\langle S_z \rangle_{calc}^{HYB}$ moments. $\langle L_z \rangle_{calc}^{HYB}$ and $\langle S_z \rangle_{calc}^{HYB}$ are similar to $\langle L_z \rangle_{calc}^{CF}$ and $\langle S_z \rangle_{calc}^{CF}$ and in agreement with $\langle L_z \rangle_{exp}$, showing that hybridization effects play also an important role in the tremendous reduction of the magnetic moments. The electronic back donation from the cage to the RE obtained with this hybridization is very small ($\sim 0.007-0.041$ electrons) compared to the transfer of three electrons from the RE to the cage. The resulting $RE^{(3-\Delta n)+}$ electronic configuration is therefore in agreement with the roughly trivalent state obtained from XAS studies. In addition, Δn decreases with the ionic radius within the RE series, following the trend that the higher the number of $4f$ electrons, the more localized the $4f$ shell and the weaker the hybridization. Secondly, the small value of Δn is surprising compared to the magnitude of momentum reduction and shows that the important feature is the spherical symmetry breaking introduced by the interaction. However, a drawback

of this hybridization model is that, even at zero temperature, the induced magnetic moment was found to vary continuously with the strength of the magnetic field simulating the Zeeman effect, while experimentally saturation was observed. But, by adding the optimal CF model discussed above to this hybridization model, the dependence of the induced moment versus magnetic field was stabilized, except again in the Gd case. Interestingly, considering both effects together gives also a good agreement with the experimental data; the shape of the obtained spectra is the same as the ones obtained with the CF term alone while t is lower than or equal to the value determined with the hybridization model alone, giving also equivalent moment reductions and back electron transfer amount. After this limit of t , the calculated spectra reproduced poorly the experiment. This shows that for Dy, Ho, and Er, the CF term is predominant on the hybridization one. But both effects are highly influencing \mathbf{L} and \mathbf{S} . The Gd case stays therefore unresolved. Only the hybridization term allows to reproduce the spin reduction that is probably at the origin of the lower μ_{eff} reported in Ref. 13. But the hybridization model we have investigated here seems too simple to prove it rigorously. More detailed models should be investigated. One possibility could be to consider an \mathbf{L} conserving hybridization term plus a CF perturbation. The hybridization term would add a $4f^8$ component to the Gd ground state, rendering it CF sensitive. However, such investigations are beyond the scope of this work.

V. CONCLUSION

The local magnetic properties of RE encapsulated in fullerenes have been studied using XMCD at 6 K with an applied magnetic field up to 7 T. The intermolecular magnetic coupling between the entrapped metal centers has been found to be paramagnetic and no magnetic anisotropy has been observed. The orbital and spin contributions of the magnetic moment have been determined through sum rules and theoretical calculations using a model Hamiltonian calculation under the effect of a perturbation. Different kinds of perturbation have been investigated: the carbon cage CF splitting of the metal orbital momentum states and some hybridization of the RE orbitals with the carbon cage orbitals resulting in an electronic back donation cage-RE. These models were based on nonspherically symmetric perturbation terms (non- L -conserving) at low interaction strengths, so low that the expectation values of $\langle L \rangle^2$ and $\langle S \rangle^2$ and their mutual alignment correspond to the pure atomic case. Both of these models considered separately allowed to reproduce the experimental spectra of Dy@C₈₂, Ho@C₈₂, and Er₂@C₉₀, whereas for Gd@C₈₂ the CF model failed and it was necessary to postulate a weak back electron donation from the cage. $\langle L_z \rangle$ and $\langle S_z \rangle$ of the encapsulated RE ions have been found significantly smaller than those of the corresponding *free* RE³⁺ ions, whatever the method used. The evolution of $\langle L_z \rangle$ and $\langle S_z \rangle$ reduction within the RE series has been found similar to the one of μ_{eff} observed by SQUID earlier¹³ but to a higher extent, especially in Gd@C₈₂ and Dy@C₈₂ cases where an anomalous branching ratio was observed. Generally this large reduction of the magnetic mo-

ments could be explained by a small CF splitting (0.2 eV) and a weak hybridization ($\Delta n = \sim 0.007-0.04$). The decrease of Δn is in agreement with the contraction of the $4f$ shell within the RE series, and resulting in a $\text{RE}^{(3-\Delta n)+}$ electronic configuration in agreement with the roughly trivalent state obtained from XAS studies. The hypothesis of a partial quenching of \mathbf{L} by the carbon cage CF cannot be retained since it would not explain the magnetic moment reduction observed for Gd, and because $\langle S_z \rangle$ is also reduced. The reduction of $\langle S_z \rangle$ can be interpreted in terms of CF taking into account the spin-orbit coupling that aligns \mathbf{S} with \mathbf{L} and the fact the electronic structure is weakly perturbed (CF perturbation remains small compared to electrostatic and spin-orbit

interactions). The hybridization model reproduces the experimental data but the failure in reproducing the observed magnetization saturation shows that it is necessary to include a CF perturbation term in the hybridization model. Finally, the carbon cage CF effect on the RE ion and the back electron donation cage-RE seems to be closely linked in the interpretation of the observed magnetic moments reduction.

ACKNOWLEDGMENT

We thank K. Larsson for his technical expertise and ESRF for excellent operating conditions.

*Present address: Diamond Light Source, Chilton, Didcot, Oxon, OX11 0QX, UK.

- ¹D.S. Bethune, R.D. Johnson, J.R. Salem, M.S. deVries, and C.S. Yannoni, *Nature (London)* **366**, 123 (1993).
- ²H. Shinohara, *Rep. Prog. Phys.* **63**, 843 (2000).
- ³B.S. Sherigara, W. Kutner, and F. D'Souza, *Electroanalysis* **15**, 753 (2003).
- ⁴D.M. Poirier, M. Knupfer, J.H. Weaver, W. Andreoni, K. Laasonen, M. Parrinello, D.S. Bethune, K. Kikuchi, and Y. Achiba, *Phys. Rev. B* **49**, 17 403 (1994).
- ⁵H. Giefers, F. Nessel, S.I. Gyry, M. Strecker, G. Wortmann, Y.S. Grushko, E.G. Alekseev, and V.S. Kozlov, *Carbon* **37**, 721 (1999).
- ⁶S. Iida, Y. Kubozono, Y. Slovokhotov, Y. Takabayashi, T. Kanbara, T. Fukunaga, S. Fujiki, S. Emura, and S. Kashino, *Chem. Phys. Lett.* **338**, 21 (2001).
- ⁷H. Shinohara, M. Inakuma, M. Kishida, S. Yamazaki, T. Hashizume, and T. Sakurai, *J. Phys. Chem.* **99**, 13 769 (1995).
- ⁸M. Takata, B. Umeda, E. Nishibori, M. Sakata, Y. Saito, M. Ohno, and H. Shinohara, *Nature (London)* **377**, 46 (1995).
- ⁹N. Lin, H. Huang, S. Yang, and N. Cue, *Phys. Rev. B* **58**, 2126 (1998).
- ¹⁰H. Funasaka, K. Sugiyama, K. Yamamoto, and T. Takahashi, *J. Phys. Chem.* **99**, 1826 (1995).
- ¹¹C.J. Nuttal, Y. Inada, Y. Watanabe, K. Nagai, T. Muro, D.H. Chi, T. Takenobu, Y. Iwasa, and K. Kikuchi, *Mol. Cryst. Liq. Cryst.* **340**, 635 (2000).
- ¹²L. Dunsch, D. Eckert, J. Froehner, A. Bartl, P. Kuran, M. Wolf, and K. H. Mueller, in *Fullerenes: Recent Advances in the Chemistry and Physics of Fullerenes and Related Materials*, edited by K. Kadish and R. Ruoff (Electrochemical Society, Pennington, 1998), Vol. 6, p. 955.
- ¹³H.J. Huang, S.H. Yang, and X.X. Zhang, *J. Phys. Chem. B* **104**, 1473 (2000).
- ¹⁴B. Kessler, A. Bringer, S. Cramm, C. Schlebusch, W. Eberhardt, S. Suzuki, Y. Achiba, F. Esch, M. Barnaba, and D. Cocco, *Phys. Rev. Lett.* **79**, 2289 (1997).
- ¹⁵O. Kahn, *Molecular Magnetism* (VCH, New York, 1993).
- ¹⁶B.T. Thole, P. Carra, F. Sette, and G. van der Laan, *Phys. Rev. Lett.* **68**, 1943 (1992).
- ¹⁷P. Carra, B.T. Thole, M. Altarelli, and X. Wang, *Phys. Rev. Lett.* **70**, 694 (1993).
- ¹⁸N. Tagmatarchis, E. Aslanis, K. Prassides, and H. Shinohara, *Chem. Mater.* **13**, 2374 (2001).
- ¹⁹N. Tagmatarchis and H. Shinohara, *Chem. Mater.* **12**, 3222 (2000).
- ²⁰H. Funasaka, K. Sugiyama, K. Yamamoto, and T. Takahashi, *J. Phys. Chem.* **99**, 1826 (1995).
- ²¹A. Mirone, M. Sacchi, and S. Gota, *Phys. Rev. B* **61**, 13 540 (2000).
- ²²B.T. Thole, G. van der Laan, and G.A. Sawatzky, *Phys. Rev. Lett.* **55**, 2086 (1985).
- ²³B.T. Thole, G. van der Laan, and P.H. Butler, *Chem. Phys. Lett.* **149**, 295 (1988).
- ²⁴G. van der Laan and B.T. Thole, *Phys. Rev. B* **43**, 13 401 (1991).
- ²⁵B.T. Thole, G. van der Laan, J.C. Fuggle, G.A. Sawatzky, R.C. Karnatak, and J.-M. Esteve, *Phys. Rev. B* **32**, 5107 (1985).
- ²⁶K. Suenaga, S. Iijima, H. Kato, and H. Shinohara, *Phys. Rev. B* **62**, 1627 (2000).
- ²⁷M. S. Golden, T. Pichler, and P. Rudolf, in *Charge Transfer and Bonding in Endohedral Fullerenes From High Energy Spectroscopy*, edited by K. Prassides (Springer-Verlag, Heidelberg, Germany, 2003).
- ²⁸H.J. Huang, S.H. Yang, and X.X. Zhang, *J. Phys. Chem. B* **103**, 5928 (1999).
- ²⁹G. Kaindl, G. Kalkowski, W.D. Brewer, B. Perscheid, and F. Holtzberg, *J. Appl. Phys.* **55**, 1910 (1984).
- ³⁰B.T. Thole and G. van der Laan, *Phys. Rev. B* **38**, 3158 (1988).
- ³¹The XAS study has been made as a function of coverages. The line shape of the white lines has been found to change from submonolayer to bulk films, reflecting an effect of either the metallic substrate or some intermolecular interactions. See http://ftp.esrf.fr/pub/UserReports/22478_A.pdf
- ³²J. B. Goedkoop, Ph.D. thesis, 1989; see also J.B. Goedkoop, B.T. Thole, G. van der Laan, G.A. Sawatzky, F.M.F. de Groot, and J.C. Fuggle, *Phys. Rev. B* **37**, 2086 (1988).
- ³³G. van der Laan and B.T. Thole, *Phys. Rev. B* **53**, 14 458 (1996).